Simulating low streamflows with hillslope storage models

Adão H. Matonse[1] and Chuck Kroll[1]

[1] In this study a deterministic approach is applied to estimate low-streamflow series and statistics at a watershed scale. The kinematic wave hillslope storage (kw) and the hillslope storage Boussinesq (hsB) models are applied in conjunction with a simple conceptual framework to a small steep headwater catchment that is part of the Maimai watersheds in New Zealand. The models are compared on the basis of their ability to reproduce base flow series and low-streamflow statistics. Variations in the number of hillslope partitions and the impact of homogeneous and variable model parameters across hillslopes are explored. Our results confirm findings from previous studies that have indicated that for steep hillslopes like those at Maimai the kw and hsB models produce similar results. More partitioning and variable parameters across the watershed can better capture hydrogeologic heterogeneity, resulting in improved model performance.

Citation: Matonse, A. H., and C. Kroll (2009), Simulating low streamflows with hillslope storage models, *Water Resour. Res.*, *45*, W01407, doi:10.1029/2007WR006529.

1. Introduction

[2] Allowable pollutant discharge concentrations are typically based on critical low-streamflow conditions specified by low-flow statistics [*Vogel and Fennessey*, 1995]. This includes the determination of Total Maximum Daily Loads for the National Pollution Discharge Elimination System (NPDES) program as defined in the Clean Water Act [*Vogel and Fennessey*, 1995; *Metcalf and Eddy Inc.*, 1991]. Low-flow statistics are also needed in water supply and irrigation planning, the determination of minimum downstream release requirements from hydropower, and the design of cooling plants and other facilities. In the United States, the most widely used indices of low flow are based on 7-day and 30-day annual minimum flow series, such as the 30-day, 2-year low flow. Parameters such as precipitation, streamflow, soil moisture, groundwater levels, moisture content in the air, and other climatic and hydrological variables have been used to characterize regional droughts, depending on the problem to be solved [*Shin and Salas*, 2000; *Eltahir*, 1992; *Frick et al.*, 1990; *Clausen and Pearson*, 1995; *Kroll et al.*, 2004]. For this study, of interest is the ability of a deterministic model to reproduce base flow series as well as the annual minimum 30-day streamflows.

[3] Low streamflows are typically due to a lack of precipitation (or immobile precipitation such as snow) and/or high evaporative losses. During these events, streamflow consists primarily of groundwater discharge [*Brutsaert and Nieber*, 1977; *Kroll et al.*, 2004], where this discharge recedes over time. Determining streamflow recession characteristics is complex because of the high variability encountered in recession behavior, both within and between catchments [*Tallaksen*, 1995]. While recession parameters are often

estimated by employing historical records, major problems arise in locations where no or reduced records of streamflow data are available. Though several methods have been developed and applied to estimate low-streamflow statistics at ungauged or partially gauged sites, such as regional regression and base flow correlation [*Stedinger and Thomas*, 1985; *Kroll et al.*, 2004; *Zhang and Kroll*, 2007a, 2007b], these methods do not provide any information about recession characteristics, and therefore cannot be used to model streamflow hydrographs. Despite our limited knowledge of what goes on underground [*Beven*, 2001], the modeling of low-flow characteristics could potentially be better simulated using physical groundwater flow models that can better adjust to changing land use and climatic patterns, and varying hydrogeology experienced in real watersheds. Low-flow conditions also represent an ideal scenario to calibrate groundwater submodels in more complex rainfall-runoff models.

[4] Groundwater models vary greatly in complexity as well as in data and computational needs. At one end of the spectrum are models based on a linear reservoir, where groundwater characteristics across a watershed are integrated into a single parameter without any consideration of the heterogeneity of the hydrologic processes involved. A linear reservoir means that groundwater discharge is modeled as a linear function of storage, resulting in an exponential decay of discharge with time. Models such as HEC-1 [*Feldman*, 1995] (note that HEC-1 is now called HEC-HMS) and GWLF [*Haith et al.*, 1992] are based on a linear reservoir approach to model groundwater. Another common technique is to assume two or more linear reservoirs to account for slower and quicker groundwater contributions, such as in SAC-SMA [*Burnash*, 1995], UBC [*Quick*, 1995], Tank [*Sugawara*, 1995], and HBV [*Bergstrom*, 1995]. These techniques, which simplify the complex heterogeneous nature of hydrogeology, are often found in rainfall-runoff models where base flow is of minimal interest. At the other end of the spectrum are fully distributed, three-dimensional models, such as MODFLOW [*McDonald and Harbaugh*,

[1]Department of Environmental Resources and Forest Engineering, State University of New York College of Environmental Science and Forestry, Syracuse, New York, USA.
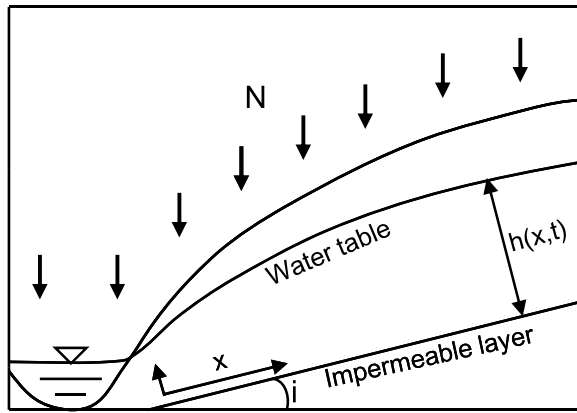
Figure 1. Schematic representation of the cross section of an aquifer overlying bedrock with constant slope angle i.

1988] or FEMWATER [*Yeh*, 1987]. These models are computationally intensive, requiring extensive data to describe the heterogeneous hydrogeologic characteristics in a region. Of interest is the development of a model that is somewhere in between these two extremes, where data needs are minimal, yet the model characterizes some of the heterogeneity of hydrogeologic processes in the watershed.

[5] This paper describes the application of a deterministic approach to simulate low streamflows at a watershed scale. Our approach is based on watershed partitioning into hillslopes and applying the kinematic hillslope storage (kw) [*Fan and Bras*, 1998; *Troch et al.*, 2002] and the hillslope storage Boussinesq (hsB) [*Troch et al.*, 2003] models. Analytical and numerical solutions to the kw and hsB models have been studied and reported in the literature. We selected hillslope storage–based models because they are physics based, are simpler than three-dimensional models, have been shown to capture the general hydrologic storage and outflow response of hillslopes with different configurations and recharge scenarios, and are generally in good agreement with the three-dimensional Richards equation [*Paniconi et al.*, 2003]. However, an analysis of previous applications of hillslope storage–based models reveals many potential limitations and questions. To begin with, applications of the kw and hsB models have been typically on synthetic hillslopes of well-defined geometry and slope profile [*Troch et al.*, 2002, 2003; *Hilberts et al.*, 2004]. In addition, only the kw model has been applied at a watershed scale, and this application required many limiting assumptions [*Fan and Bras*, 1998]. *Troch et al.* [2003] show how results from the kw model differ from those of the hsB model for convergent hillslopes, and that these differences become insignificant for steep, divergent, or fast draining hillslopes. Of interest here is to what extent these hillslope differences impact streamflow discharge simulation at a watershed scale. Also, there are currently no examples of application of the hsB model at a watershed scale. Here we compare the kw and hsB models at a watershed scale to simulate base flow dynamics at Maimai catchment M8 on the southern island of New Zealand. Our primary objectives are to (1) develop a model framework, (2) examine how model performance changes as the range of data employed for model calibration varies, and (3) analyze how the model calibration process evolves to better fit the observed stream-

flow data, given the use of kw and hsB models, varying degrees of watershed partitioning into hillslopes, and the use of uniform versus variable parameters across the study area.

2. Kinematic Hillslope Storage and the Hillslope Storage Boussinesq Models

[6] Partially saturated hillslope subsurface drainage can be described by the Richards equation [*Brutsaert and El-Kadi*, 1984]. Since the resulting solutions of this equation cannot easily be parameterized, a hydraulic approach is often taken [*Brutsaert*, 1994]. Assuming negligible evapotranspiration and capillary effect, Boussinesq derived an expression for one-dimensional flow from an unconfined sloping aquifer [*Childs*, 1971]. Combining this with the continuity equation one obtains the Boussinesq equation:

$$\frac{\partial h}{\partial t} = \frac{k}{f}\left[\cos(i)\frac{\partial}{\partial x}\left(h\frac{\partial h}{\partial x}\right) + \sin(i)\frac{\partial h}{\partial x}\right] + \frac{N}{f} \qquad (1)$$

where $h = h(x,t)$ is the elevation of the groundwater table measured orthogonally to an impermeable bed with slope i, f is the drainable porosity, k is the hydraulic conductivity, and N represents the rainfall recharge to the groundwater table. Equation (1) is based on the assumption that k, f, and i are constant, and can be applied to estimate subsurface flow along a unit-width hillslope (Figure 1).

[7] Equation (1) is limited to one-dimensional groundwater flow, and therefore does not account for the three-dimensional characteristics of the aquifer. In addition, when dealing with complex hillslopes it does not capture the effect of hillslope geometry, which may be one of the most important factors that control subsurface flow [*Troch et al.*, 2002, 2003; *Hilberts et al.*, 2004]. *Fan and Bras* [1998] introduced a new approach based on using a soil moisture storage capacity function to incorporate topographic and geometric aspects that control flow processes at a hillslope scale. By introducing the soil moisture storage capacity function, $S_c(x)$, which defines the thickness of the pore space along the hillslope, *Fan and Bras* [1998] presented a method to simplify the three-dimensional soil mantle into a one-dimensional profile. This approach accounts for both the plan curvature, defined by a hillslope width, $w(x)$, and profile curvature, defined by an average maximum soil depth, $\overline{d}_m(x)$:

$$S_c(x) = w(x)\overline{d_m}(x)f \qquad (2)$$

At any time at a given location the storage content $S(x,t) \le S_c(x)$. This formulation assumes that the plan shape and the profile curvature are the dominant topographic factors that control flow processes along a hillslope. *Fan and Bras* [1998] and *Troch et al.* [2002] combined a kinematic wave (kw) approximation of Darcy's law:

$$Q = -k\frac{S(x,t)}{f}\frac{\partial z}{\partial x} \qquad (3)$$

where z is the elevation of the bedrock above a base datum, with the continuity equation:

$$\frac{\partial S(x,t)}{\partial t} + \frac{\partial Q}{\partial x} = N(t)w(x) \qquad (4)$$

to derive a quasi-linear equation solvable by the method of characteristics. For a given recharge $N(t)$, and constant hydraulic conductivity k, they derived the following hillslope storage equation:

$$a(x)\frac{\partial S(x,t)}{\partial x} + \frac{\partial S(x,t)}{\partial t} = c(x,S),\tag{5}$$

where $a(x) = -\frac{kz'(x)}{f}$,

$$c(x,S) = N(t)w(x) + \frac{kz''(x)}{f}S(x,t),$$

and $z'(x)$ and $z''(x)$ are first and second derivatives of the bedrock profile curvature function $z(x)$, respectively. To describe the bedrock profile curvature *Fan and Bras* [1998] adopted a second-order polynomial function, while in this study we follow the method of *Troch et al.* [2002] who used a power function from *Stefano et al.* [2000] (as cited by *Troch et al.* [2002]) that has the form:

$$z(x) = E + H\left(\frac{x}{L}\right)^n + \varepsilon y^2\tag{6}$$

where E is a reference datum (equals zero at the outlet), H is the elevation above the datum of the bedrock along the hillslope, L is the slope length, n defines the profile curvature, ε accounts for the plan curvature, and y is the distance from the slope center perpendicular to the x axis. For $n > 1$ the profile is concave, for $n < 1$ convex, and for $n = 1$ the profile is linear. For simplicity in this study ε is always set to zero, meaning that the hillslope is not curved in the y direction. This formulation, further referred to as the kinematic wave hillslope storage model (or simply as the kw model), can be solved numerically by using equation (5) and discretizing the storage in time and space.

[8] Because of the kinematic wave approximation the kinematic model is valid only for moderate to steep slopes. *Troch et al.* [2003] expanded the hillslope storage equation to achieve a more general formulation, which could be applied to a full range of slopes. By adopting a more general form of Darcy's law:

$$Q = -\frac{kS(x,t)}{f}\left[\cos i\frac{\partial}{\partial x}\left(\frac{S(x,t)}{fw(x)}\right) + \sin i\right]\tag{7}$$

the new formulation accounts for diffuse and gravity drainage, and has the form:

$$f\frac{\partial S}{\partial t} = \frac{k\cos i}{f}\frac{\partial}{\partial x}\left[\frac{S(x,t)}{w(x)}\left(\frac{\partial S(x,t)}{\partial x} - \frac{S(x,t)}{w(x)}\frac{\partial w(x)}{\partial x}\right)\right]$$
$$+ k\sin i\frac{\partial S(x,t)}{\partial x} + fN(t)w(x)\tag{8}$$

In synthetic hillslopes with homogeneous soil characteristics, equation (8) has been shown to produce results similar to the three-dimensional Richard's equation [*Paniconi et al.*, 2003]. In the present analysis this formulation, referred to here as the hillslope storage Boussinesq (hsB) model, is applied and compared to the kw model. The hsB model becomes a kw approximation under relatively steep impermeable bed slopes where it is assumed that the rate

of groundwater flow is relatively high. As a consequence, the flow streamlines in a saturated soil mantle are parallel to the slope of the impermeable layer and the hydraulic gradient at any point within the saturated zone is equal to the bed slope [*Wooding and Chapman*, 1966; *Chapman*, 1995; *Beven*, 1981]. Under these assumptions the second-order diffusive term in equation (7) can be dropped. equation (8) can be solved numerically by discretizing the solution space, using an explicit finite difference approximation, and applying an ordinary differential equation (ODE) solver in time. This solution can accommodate different boundary conditions, as well as the temporal and spatial variability of recharge, hydraulic parameters, and slope angle.

[9] Here the hydraulic conductivity is assumed to vary as power function of the storage deficit, defined as the total storage at the beginning of each time step divided by the total storage capacity. We follow the power function approach used by *Rupp and Selker* [2006] with the form:

$$k(z) = k_D(z/D)^\mu\tag{9}$$

were D is the depth of the soil mantle, k_D is the saturated hydraulic conductivity at height z = D, and μ is a (calibrated) constant greater or equal to zero. We substituted (z/D) with the storage deficit. For the finite difference discretization we selected the size of the space and time increments (Δx and Δt, respectively) to preserve the von Neumann conditional stability bound [*Huyakorn and Pinder*, 1983; *Wang and Anderson*, 1982]:

$$k\cos i\frac{\Delta t}{f^2\Delta x^2} \le 0.5\tag{10}$$

to ensure stability of the numerical solution. The mixed boundary conditions (a combination of Dirichlet and Neumann boundary conditions) are set as S = 0 at the hillslope outlet and $\partial S/\partial x = 0$ at the upslope boundary. Though the assumption of S = 0 is unrealistic for groundwater flow on a hillslope where a seepage face is expected, this assumption creates difficulty in calculating discharge at the lower boundary from Darcy's law [*Beven*, 1981]. Using a numerical solution and estimating the discharge based on mass conservation, this assumption has little impact on estimated flow rates [*Beven*, 1981]. Initial soil moisture content across the watershed is set by calibration.

3. Study Site

[10] The Maimai watersheds were established as research sites in 1974 by the New Zealand Forest Research Institute, and are part of the Tawhai State Forest, near Reefton, North Westland, on the South Island of New Zealand. Maimai has been the subject of several hillslope and catchment-based hydrological studies, examining subwatersheds ranging in size from 1.63 to 280 ha [*McGlynn et al.*, 2002, 2004; *Weiler et al.*, 2003]. Recently *Lyons and Troch* [2007] examined the use of a subsurface flow similarity index, derived from analytical solutions to a linearized version of hsB, at a number of Maimai subwatersheds. In this study we employ the 3.8 ha Maimai catchment M8, a well-studied headwater catchment with relatively homogeneous hydrologic

Table 1. Observed Annual Totals for P and Q and Annual Estimates for ET and L

Year	Rainfall (mm)	Discharge (Q) (mm)	ET (mm)	Losses to Regional Groundwater System (L)
1986	2190	1285	837	84
1987	2246	1311	837	86
1988	2668	1757	837	103

characteristics, and a good (albeit short) record of precipitation, temperature, and streamflow.

[11] Average gross annual precipitation in the study area is approximately 2600 mm, resulting in 1550 mm of runoff [*Rowe*, 1979; *Freer et al.*, 1997; *McDonnell*, 1990]. Soils are shallow with an average depth of 60 cm, including a well developed 17 cm organic soil horizon and a very friable mineral layer of podsolized, stony subsoil, predominantly of silt loam textures [*McGlynn et al.*, 2002]. Soil depth is highly variable in M8, and is thus calibrated in our experiment. The organic humus exhibits a mean total porosity of 86% by volume, 39% macroporosity, and an average infiltration rate of 6100 mm/h [*McGlynn et al.*, 2002; *McGlynn*, 2002; *McDonnell*, 1990]. The mineral soils are very permeable with total porosity of 45% by volume, average bulk densities of 1.5 mg/cm^3, and saturated hydraulic conductivities varying between 10 and 300 mm/h [*McGlynn*, 2002]. The soils in M8 overlay Old Man Gravels, a less permeable early Pleistocene well-cemented conglomerate of clasts of sandstone, granite, and schist in a clay-sand matrix [*McGlynn et al.*, 2004]. Losses to deep groundwater are estimated to be 100 mm/a [*McGlynn et al.*, 2002]. This value divided by the average annual precipitation (100/2600 = 3.8%) was used as a precipitation loss ratio to deep percolation in this study. Annual interception losses over the study area average 26% of total precipitation for the undisturbed mixed evergreen forest found in M8 [*Rowe*, 1979; *McGlynn et al.*, 2002]. The hillslopes are relatively short in length (less than 300 m) but steep (34°), and composed of regular spurs and linear hollows. The combined effect of topography and soil characteristics results in strongly weathered and leached soils, with high moisture content (within 10% of saturation for most of the hydrologic year) and low natural fertility. Runoff production over M8 is extremely rapid via macropores and groundwater dynamics that dominate the basin response during storm events [*McDonnell*, 1990]. The existence of macropores and preferential flow paths could represent a potential problem for applying Darcy's law, which is based on a representative continuum of the porous media where flow takes place [*Freeze and Cherry*, 1979; *Snow*, 1969]. For the purpose of the present work, we did not emphasize the impact of macropores. Our assumption was that under low-streamflow conditions the impact of existing preferential flow paths is minimal and can be captured by effective values of model parameters.

4. Going From Hillslope to Watershed Scale: A Simple Modeling Framework

[12] *Fan and Bras* [1998] applied the kw model at a watershed scale. Some disadvantages with their approach include the appropriateness of the kinematic solution for only moderate to steep slopes, and the use of rainfall directly as recharge, neglecting other processes such as evapotranspiration and interception. In order to address some of these limitations, we have accounted for evapotranspiration and interception in the watershed. Storm response by saturation excess runoff accounts for a small amount of streamflow [*Mosley*, 1979; *Pearce et al.*, 1986] and since we are primarily interested in reproducing base flow series and statistics, we also neglected infiltration excess surface runoff. To estimate recharge to groundwater across the watershed and preserve the overall mass balance, the discharge at the outlet of each hillslope was estimated for each time step as:

$$Q_T = S_{T-1} - S_T + R - L \qquad (11)$$

Where Q_T is the discharge, S_{T-1} is the total (volumetric) storage at the end of the previous time step, S_T is the total storage at the end of the present time step, R is the total recharge, and L represents losses to deep percolation. Recharge is estimated from precipitation (P) after subtracting evapotranspiration (ET), and interception (I):

$$R = P - ET - I \qquad (12)$$

Values for P and ET were available at an hourly and daily basis, respectively, where ET was obtained by fitting a sine curve to average monthly potential evapotranspiration values estimated as the average of monthly estimates from five different models [*Rowe et al.*, 1994]. Negative R was allowed to account for losses in soil moisture in the absence of rainfall. Model simulations were performed at an hourly time step. While for larger watersheds it is necessary to route streamflow contributions from individual hillslopes to the watershed outlet, in a small watershed such as M8 the time of concentration is less than model time step and routing is unnecessary.

5. Model Requirements

5.1. Input Data

[13] Available data for the M8 watershed includes hourly P, Q, and daily ET for 3 years (January 1986 to December 1988). Table 1 represents the observed and estimated annual totals for these values, as well as the estimated losses to the deep groundwater system in each year.

5.2. GIS Preprocessing and Hillslope Delineation

[14] GIS preprocessing was employed to partition the watershed into hillslopes. Here we followed the empirical approach using the same methodology described by *Fan and Bras* [1998]. Hillslopes were classified as straight, convergent, or divergent, or a combination of these shapes, on the basis of the general flow line patterns [*Paniconi et al.*, 2002; *Troch et al.*, 2002; *Fan and Bras*, 1998]. Areas with similar hillslope characteristics were aggregated to form larger hillslopes, and width function parameters were chosen to preserve the surface area of the hillslopes. Figures 2a and 2b represent the Maimai M8 DEM with elevation contour lines and the

a) 3 hillslope partition   b) 10 hillslope partition
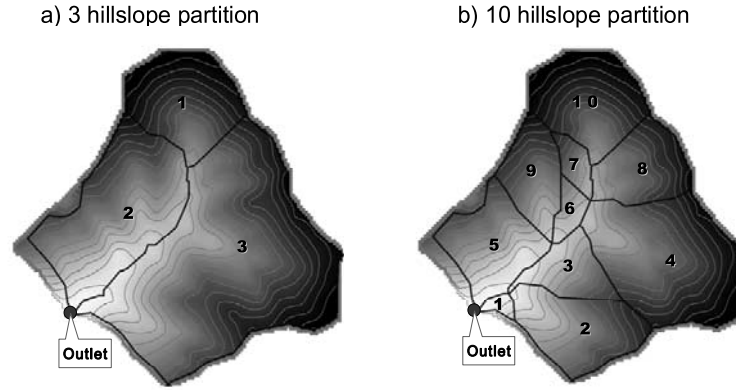
Figure 2. Maimai M8 catchment DEM with three and ten hillslopes partitions. Dark colors represent areas with higher elevations, and light colors represent areas with lower elevations.

hillslopes for 3 and 10 partitions, respectively. Higher elevations exhibit a dark color, while low elevations have a lighter color. Table 2 presents hillslope parameters.

5.3. Model Parameter Estimation (Calibration) and Model Comparison

[15] The Shuffled Complex Evolution (SCE) [*Duan et al.*, 1993] algorithm was applied to calibrate hydraulic conductivity, soil porosity, soil depth, initial soil moisture content at the beginning of the simulation period, and constant μ from equation (9). Table 3 represents the ranges set for each parameter during the calibration procedure. These ranges were defined on the basis of M8 literature values and enlarged to allow more flexibility during the calibration procedure. In addition to the use of the full range of data for model calibration, we also calibrated the models using only data lower than the 20th and 50th streamflow percentiles. This was done to evaluate how restricting the range of calibration data impacts the model's ability to simulate low streamflows.

[16] Model calibration was performed at a daily time step by minimizing a scaled root-mean-square error

$$SRMSE = \left[\frac{(n-1)}{n} \frac{\sum_{i=1}^{n} (O_i - S_i)^2}{\sum_{i=1}^{n} (O_i - \overline{O})^2} \right]^{\frac{1}{2}} \qquad (13)$$

where $\overline{O}$ is the mean of the observed values, O_i and S_i are the observed and simulated streamflows at time i, respectively, and n is the number of streamflows. SRMSE represents the RMSE divided by the standard deviation of the observed streamflows over the calibration range. For a calibration stopping criteria we applied a method of function convergence [*Sorooshian and Gupta*, 1995]:

$$(SRMSE_{i-1} - SRMSE_i)/SRMSE_i \leq \varepsilon_f \qquad (14)$$

where $SRMSE_{i-1}$ and $SRMSE_i$ are the best SRMSE values from the previous and current iteration steps, respectively, and ε_f is a defined convergence criterion. During our model calibration we set ε_f equal to 10^{-4}.

[17] SRMSE was also applied to evaluate model performance at lower ranges of streamflow data. The scaling of RMSE reduces the impact of different ranges of streamflow data used during model calibration and produces a better comparison of the results from different simulations. To compare models performance over the full streamflow hydrograph for the different simulations, the Nash-Sutcliffe efficiency coefficient [*Nash and Sutcliffe*, 1970] defined as:

$$R_{eff} = 1 - \frac{\sum_{i=1}^{n} (O_i - S_i)^2}{\sum_{i=1}^{n} (O_i - \overline{O})^2} \qquad (15)$$

was applied. While we focus on the simulation of streamflows at lower ranges, it is important to know how the models capture the full hydrograph. R_{eff} measures the proportion of variance in the observed data accounted for by the model and is a function of the SRMSE. We use R_{eff} in the next section to compare our results with those of *Seibert and McDonnell* [2002] who employed a three-box model to M8. We also compare the observed and simulated annual

Table 2. Fixed Hillslope Parameters for One, Three, and Ten Partitions of the M8 Watershed

Hillslope	Single Partition Basin	Three Partition Basin			Ten Partition Basin									
		1	2	3	1	2	3	4	5	6	7	8	9	10
Slope (deg)	34	34	34	34	26	34	33	34	34	29	37	35	35	34
Length (m)	216	93	73	135	30	119	77	147	71	19	32	78	109	93
Area (ha)	3.8	0.57	1.00	2.23	0.04	0.52	0.26	1.01	0.49	0.09	0.10	0.39	0.33	0.57

Table 3. Upper and Lower Limits for Calibrated Parameters

Parameter Name	Lower Limit	Upper Limit
Hydraulic conductivity (m/h)	0.0001	10.0
Soil porosity	0.2	0.9
Soil depth (m)	0.07	2.0
Initial soil moisture	0.05	1.0
Power exponent	0.0	15.0

minimum 30-day statistics (Q_{30}), which is often employed in low-streamflow analyses.

6. Results and Discussion

6.1. Comparing Kinematic and hsB Models Against the Three-Box Model

[18] An initial analysis compares our hillslope based approach to a model previously applied to M8, the three-box model developed by *Seibert and McDonnell* [2002]. The three-box model is a site specific model that combines three reservoirs representing the riparian, hollow, and hillslope zones across the M8 catchment. The three-box model includes a total of 16 parameters when calibrated using runoff data and groundwater level series (hard data as referred to by the authors). This number of parameters increases when additional soft data are used during model calibration with the objective of guiding the parameter search process and improving the model's ability to describe certain characteristics inside each box. The reason for this comparison is to determine how our approach of watershed partitioning into hillslopes compares to a model based on a series of linear reservoirs. Seibert and McDonnell simulated daily streamflow discharge for the M8 catchment over a 5-month period between August and December 1987. Though this period is relatively short, we applied both the kw and hsB models for the same period with M8 described as one hillslope (five parameters), partitioned into three hillslopes with uniform parameters (5 parameters), and partitioned into three hillslopes with variable parameters (13 parameters). Table 4 shows the comparison between R_{eff} for the four models. On the basis of R_{eff} (which was employed by Seibert and McDonnell), our 1 and three hillslope models with five uniform parameters produce $R_{eff} = 0.94$ and $R_{eff} = 0.95$, respectively, and perform as well as the 16 parameter three-box model ($R_{eff} = 0.93$). The kw and hsB models with three hillslope partition and variable parameters exhibit an even higher performance in simulating daily streamflows with $R_{eff} = 0.98$ and 0.97, respectively.

[19] In Figure 3 the hydrographs between the modeled and observed streamflows for the period between August and December 1987 are presented. In general the model with one hillslope overestimates the peak streamflows during larger storm events when compared with the three hillslope model, indicating that partitioning allows model flexibility that resulted in better simulation of streamflows over all ranges. Both models seem to underestimate low-flow recession events.

[20] As our interest is low-streamflow simulation, an analysis of recession slope curves [*Rupp and Selker*, 2006] is warranted. *Brutsaert and Nieber* [1977] presented three different analytical solutions to the Boussinesq equation for unconfined flow in a homogeneous horizontal aquifer with a uniform hydraulic conductivity. The two exact solutions [*Boussinesq*, 1904; *Polubarinova-Kochina*, 1962] and one approximation by linearization [*Boussinesq*, 1903], can be presented in following form:

$$-\frac{dQ}{dt} = aQ^b, \qquad (16)$$

were a is a function of physical and hydraulic properties of the aquifer and b is a constant. Plotting $log\,(-dQ/dt)$ versus $log\,(Q)$, the above recession slope curve results in straight line with slope b and intercept $log(a)$. For the linear solution $b = 1$ [*Vogel and Kroll*, 1992], while for the exact solutions $b = 3$ for early times and $b = 1.5$ for later times [*Brutsaert and Nieber*, 1977].

[21] *Rupp and Selker* [2006] extended this analysis to address issues with a sloping aquifer and a varying hydraulic conductivity with depth. For their analysis *Rupp and Selker* [2006] applied numerical solutions to the full nonlinear Boussinesq equation and used a power law in equation (9) to express vertical variations of the hydraulic conductivity across the soil mantle. For a sloping aquifer, the analytical solutions to the linearized one-dimensional Boussinesq equation is inappropriate for recession slope analysis, while new empirically derived solutions appears to be more [*Rupp and Selker*, 2006]. Figure 4 shows the recession slope curve for M8 streamflow data for the same period as in the work by *Seibert and McDonnell* [2002]. The analysis follows the *Brutsaert and Nieber* [1977] method assuming a 3-day moving average [*Kroll et al.*, 2004]. The recession slope analysis estimated $b = 1.44$, which is within the range for most studies with sloping aquifers [*Rupp and Selker*, 2006] and consistent with a nonlinear Boussinesq solution [*Brutsaert and Nieber*, 1977].

6.2. Kinematic Versus hsB Models With a Single Hillslope

[22] Assuming that a hillslope-based method represents a valid alternative to simulating low streamflows, our first

Table 4. Comparison of Model Performance for Daily Streamflows for August Through December 1987

	Seibert and McDonnell [2002]: Three-Box Model	One Hillslope Partition		Three Hillslope Partition: Uniform Parameters		Three Hillslope Partition: Variable Parameters	
		Kinematic Model	hsB Model	Kinematic Model	hsB Model	Kinematic Model	hsB Model
Nash-Sutcliffe coefficient	0.93	0.94	0.94	0.95	0.95	0.98	0.97
Total number of calibration parameters	16	5	5	5	5	13	13
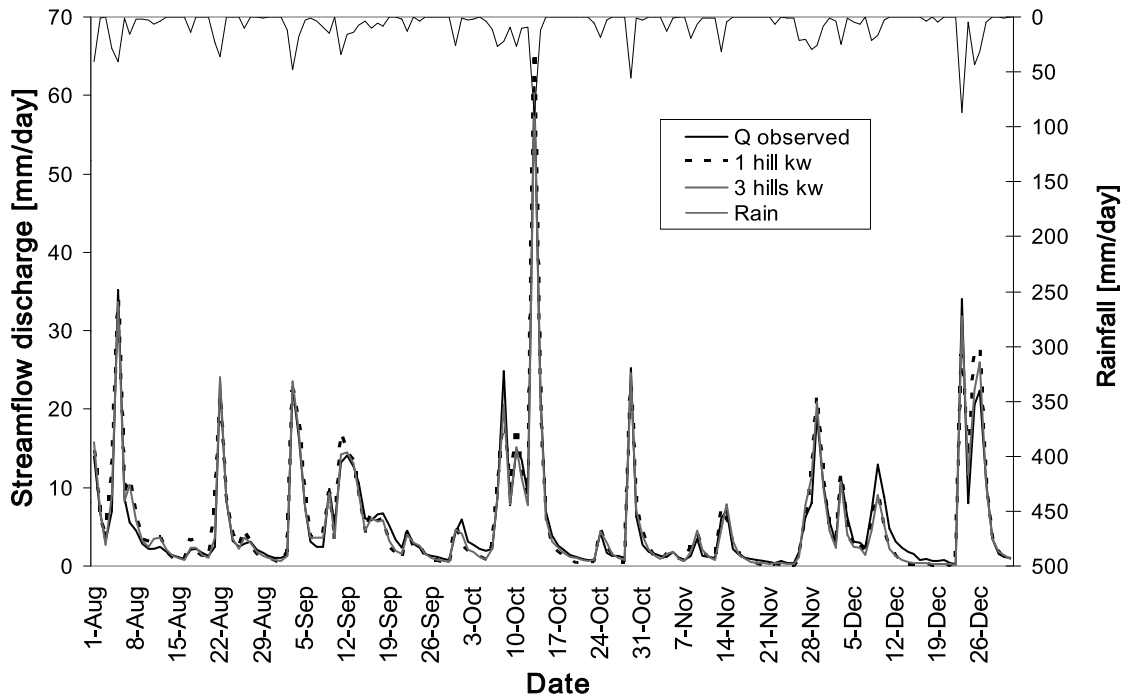
Figure 3. Comparison between observed and modeled daily flow hydrographs for M8: August–December 1987.

comparison is between the kw and the hsB models with M8 represented as a single hillslope. During our model simulations the kw and hsB models were run on an hourly time step while calibrated to fit daily streamflow data. Initially, we calibrated our models to fit the full range of observed streamflow data, and results are presented in Table 5. The kw and hsB models have similar performance when describing observed data over the full range of streamflow. When calculating the performance metrics on a daily time scale as opposed to an hourly time scale, both models improve drastically as there is a smoothing of the model response over a longer time scale.

[23] For the estimation of low-streamflow statistics, though, we are not interested in predicting the full range of observations but instead only the smaller values. To address this issue, SRMSE and R_{eff} were also calculated for the lowest 50th and 20th percentile of the observations

for the models calibrated using the full range of data. These results are also presented in Table 5, and show an enormous drop in model performance for both models. This result raises two important issues. The first is that one needs to be very sensitive to model objectives, since if the range of data employed for model calibration has a different magnitude than the data employed for model performance, results may be poor. The second issue is the use of R_{eff} for model performance, which can become inflated when a small number of large values are present in the data set, as is common with streamflow data. For simplicity and for the remainder of this paper, we will use daily streamflow data and R_{eff} to represent model performance over the full range of data, and SRMSE to compare model performance over lower-streamflow ranges. We choose R_{eff} for the full range because it allows comparison with results from previous studies at M8 [*Seibert and McDonnell*, 2002], and selected SRMSE for evaluating model performance at lower ranges because with reduced amounts of data at lower ranges R_{eff} results in low values which are difficult to compare.
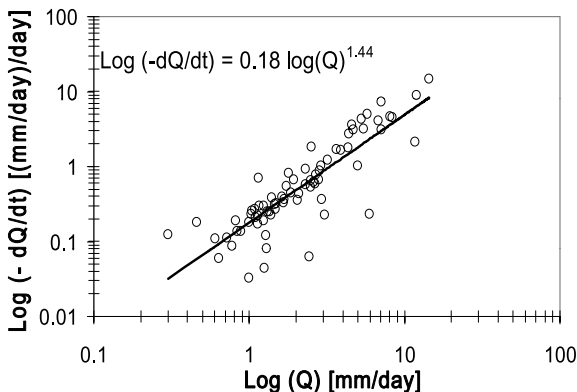
Figure 4. Recession slope plot for daily streamflow data: August–December 1987.

Table 5. Scaled Root-Mean-Square Error and Nash-Sutcliffe Efficiency for the kw and hsB Models Calibrated Using the Full Range of Data[a]

| | Data Range Applied for the Performance Metric | | | | | |
| | Full Range | | Lower 50% | | Lower 20% | |
	kw	hsB	kw	hsB	kw	hsB
R_{eff} daily	0.88	0.89	0	0	0	0
SRMSE hourly	0.8	0.8	3.8	4.1	6.5	7.2
SRMSE daily	0.4	0.3	2.2	2.0	4.0	3.7

[a]Performance metrics was calculated for the full range of data, and the lower 50 and 20%. Abbreviations are as follows: SRMSE, scaled root-mean-square error; R_{eff}, Nash-Sutcliffe efficiency.
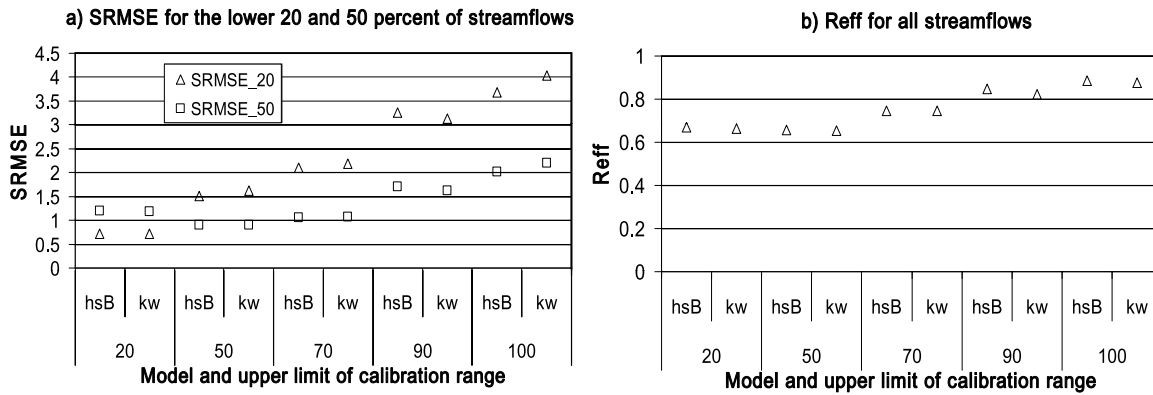
Figure 5. SRMSE and R_{eff} with one hillslope kw and hsB models calibrated using varying ranges of streamflow.

[24] On the basis of these results, an experiment was performed to analyze the impact of the calibration range on model performance. Both models were calibrated using the lowest 20th, 50th, 70th, and 90th percentiles of streamflow, and over the full range of observed daily streamflow data, and performance statistics were calculated for daily estimates employing only data below the 20th, 50th, and 100th percentiles. Calibration on a lower percentile means that while the model is run to simulate the full range of data, the objective function for the calibration process is calculated using only observed data below the percentile threshold and their corresponding (same date and time) simulated data. Lower percentiles for both calibration and performance statistics were set using observed data. Figure 5a shows the SRMSE results for the lower 20 and 50% of streamflow data. The performance between the kw and hsB models is similar across all calibration ranges. As expected, models calibrated using the lower 20% of data show the best SRMSE for the lower 20% range of data, while models calibrated using the lower 50% of data show the best SRMSE for the lower 50% range of data. In general SRMSE increases as the calibration range increases reflecting model difficulty in simulating a lower range while trying to fit to higher streamflow values. Calibration using the lowest 50th percentile of the data as opposed to the full range has the impact of removing the largest streamflow observations from the calibration and results in a large drop in SRMSE, again indicating an adverse impact of calibrating with large streamflow values when one is interested in reproducing low streamflows. Figure 5b shows the R_{eff} values over all streamflows when models are calibrated over reduced ranges of streamflow. Again the kw and hsB models are similar in performance. R_{eff} values over the entire flow hydrograph increase with an increase in the calibration range. When the calibration range is reduced, the ability of the models to reproduce the entire hydrograph is also reduced.

[25] In Figure 6 we present how the kw and hsB models predict the 30-day annual minimum streamflow (Q_{30}) as the ratio between simulated divided by observed Q_{30}. The kw and hsB models perform similarly. All models perform well in predicting Q_{30} for the relatively wet year (1988) than for the relatively dry year (1987). Q_{30} for 1988 is 0.98 mm/d which is the 41st percentile of streamflow, while Q_{30} for 1987 is 0.32 mm/d and is the 17th percentile of streamflow.

For the dry year all models overestimate Q_{30}, indicating a drop in model performance for extremely low streamflows. Models calibrated with the lower 20 and 50% of streamflow produce the best simulated values. Results (not presented) also showed that all models systematically overestimate Q_7. Q_7 values are very small, equivalent to the 1st percentile of streamflow. In addition M8 has a relatively short streamflow record length and thus has limited data to calibrate to such small values. Under these circumstances the simulation of Q_7 is difficult, and for these reasons we decided not to include the results in this paper.

[26] There are two important lessons from this initial analysis. The first is that because of relatively steep average slopes in M8 the results for both the kw and hsB models are similar when M8 is modeled as a single hillslope. This can be explained not only by the slope characteristic but also from the complex shape of the overall hillslope, which is more like a combination of hillslopes of multiple shapes. The second lesson is that the data employed for calibration greatly impacts model performance. If one is interested in simulating streamflow over a narrow range of discharge (such as in reproducing low streamflows), the data employed to calibrate the model should also be similar to that range. The problem is that in doing so, you may considerably reduce the amount of data available for calibration, as well
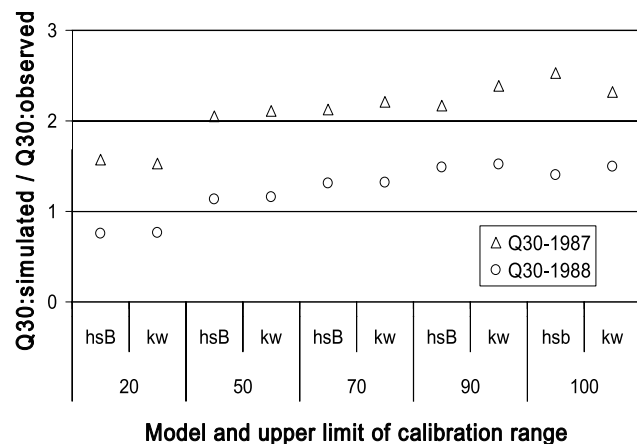
Figure 6. Simulated divided by observed Q_{30} with one hillslope kw and hsB models calibrated using varying ranges of streamflow.

a) SRMSE for the lower 20 and 50 percent of streamflows

△ 1 hill　□ 3 hills uni　○ 10 hills uni　■ 3 hills var　● 10 hills var

b) Reff for all streamflows
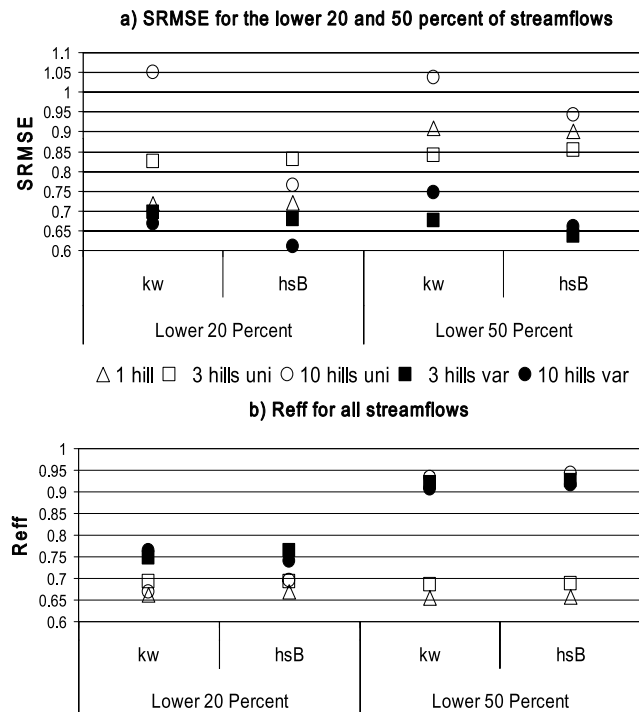
Figure 7. SRMSE and R_{eff} with kw and hsB models calibrated using uniform and variable parameters and varying hillslopes and ranges of streamflow.

as impact how your models reproduce other summary statistics.

6.3. Modeling With Single Versus Multiple Hillslope Watershed Partitions With Uniform Parameters

[27] In this section we present the model results with M8 partitioned into multiple hillslopes, but the calibrated parameters are assumed to be uniform (homogeneous) across hillslopes over the entire watershed. This analysis allows us to investigate the impact of changing hillslope configurations as opposed to changing hillslope parameters. For this and all subsequent analyses, we will calibrate and calculate performance statistics (SRMSE) using the same data range; that is, performance statistics for the lowest 20 and 50% of the data are calculated from simulations calibrated with data below the 20th and 50th percentiles, respectively.

[28] In addition we provide R_{eff} over the full range of streamflow for models calibrated over a lower range to gain a sense of how these models simulate the entire hydrograph when trying to fit streamflows at a lower range, and thus these results can be compared to results in section 6.2. Figure 7a presents the SRMSE for the kw and hsB models with uniform parameters (nonfilled symbols). The results indicate that models with multiple hillslopes with uniform parameters do not perform better than one hillslope models when simulating data for lower ranges. This may be due to employing uniform model parameters across hillslopes, which may limit the flexibility of simulations with multiple hillslopes.

[29] For the R_{eff} values in Figure 7b all models calibrated using the lower 20% of data perform similarly in describing the full hydrograph. Interestingly the ten hillslope models

with uniform parameters calibrated with the lower 50% of streamflow does much better over the full range, while performing poorly for simulating the lower range of streamflow. This indicates this model provides more flexibility in describing hydrologic process across the entire range of streamflow.

[30] Estimates of Q_{30} for each year are presented in Figure 8 and show a mixed behavior. In general all models simulate Q_{30} well for the wet year (1988), but perform poorly for the relatively dry year (1987). As with SRMSE, Q_{30} shows no advantage for hillslope partitioning with uniform parameters when compared to one hillslope models.

[31] Advantages associated with multiple hillslopes include a better representation of surface topography and flow dynamics, as well as better representations of slope variations across the watershed. Slopes in M8 are in general steep but short in length, and soil properties such as the hydraulic conductivity are also highly variable [*McDonnell*, 1990]; under these circumstances multiple hillslopes are warranted but uniform parameters may restrict model flexibility to adjust to varying watershed properties.

6.4. Variable Versus Uniform Model Parameters for Multiple Hillslopes

[32] To test the impact of variable versus uniform parameters on model performance, model parameters for each hillslope were allowed to vary. We used Figures 7a, 7b, and 8 to present the resulting SRMSE, R_{eff}, and Q_{30}, respectively, for the models with variable and uniform parameters.

[33] Figure 7a shows that hillslope partitioning associated with variable parameters leads to better model performance at both ranges, though this improvement is small for some situations. When using variable parameters, further partitioning from three to ten hillslopes does not produce different results, suggesting that the three hillslope models associated with variable parameters have enough flexibility to perform as well as models with more hillslopes. This overall improvement with partitioning and variable parameters is also reflected in R_{eff} over the entire streamflow hydrograph (Figure 7b). Variable parameter models and the ten hillslope uniform parameter model calibrated using the lower 50% of streamflow exhibit a much better performance over the full range of streamflow. Models using variable parameters better simulate the entire streamflow hydrograph
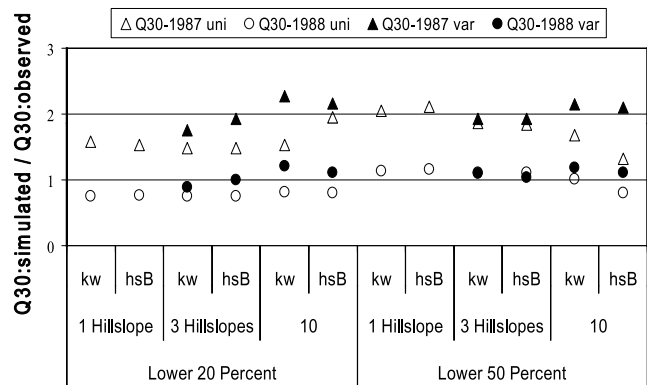
Figure 8. Simulated divided by observed Q_{30} with kw and hsB models calibrated using uniform and variable parameters and varying hillslopes and ranges of streamflow.
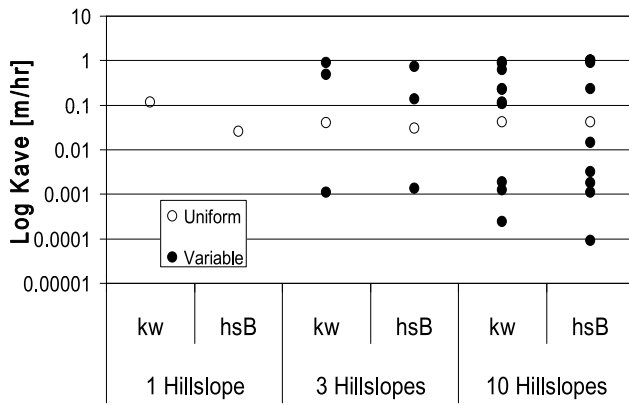
Figure 9. Average hydraulic conductivity (Kave) for kw and hsB models calibrated using the lower 20% of streamflow data.

while still having the lowest SRMSE over the 50% calibration range. Results over the 20% range, which show little difference between all models, may be affected by the limited data available for model calibration.

[34] In Figure 8 models with variable parameters do better in simulating Q30 for the wet year (1988), while models with uniform parameters do better for the dry year (1987). As stated before, since Q30 for the dry year represents a very low streamflow percentile compared with the upper limits of the calibration range, the models show a reduced ability to simulate the lower range of streamflow data.

[35] The overall lower SRMSE combined with relatively high R_{eff} values and better Q_{30} for simulations with varying parameters suggest that even for a relatively small and homogeneous watershed such as M8, having multiple partitions and varying watershed characteristics allows hillslope models to better simulate lower streamflow values.

[36] *Bogaart and Troch* [2004] analyzed results from a simulated watershed and concluded that the composite hydrograph of a partitioned watershed is more similar to that of a uniform hillslope, because of the compensating effect between convergent and divergent hillslopes. With more hillslopes this is more likely to occur. Also, they related shallow base flow to drainage of relatively wet upslope areas, which are often connected to convergent hillslopes. The implication of this analysis is (1) the kw model may perform poorly in watersheds with predominantly convergent hillslopes; (2) watershed partitioning with multiple hillslopes of varying shape will improve the kw model because of the compensating effect between convergent and divergent hillslopes in the composite hydrograph; (3) the hsB model should produce better results for low streamflows in a predominantly convergent watershed; and (4) where the impact of diffuse drainage is insignificant, the performance of both the kw and hsB models should be similar. Though the present work confirms some of these conclusions, our results are limited because of the small amount of data available for this study.

6.5. Model Parameter Behavior: Hydraulic Conductivity

[37] In this final section we examine how changes in calibrated hydraulic conductivity (k) vary as the number of

hillslope partitions change, as well as having uniform or variable parameters when multiple hillslopes are employed. While other model parameters are also calibrated, k is particularly of interest because it not only has a large impact on hillslope drainage, but also has been estimated by other researchers who have worked at this study site. Because k is modeled to vary with depth (equation (9)), calibrated values represent k for full saturation at the surface. These values are most representative during larger storm events, and less representative during low streamflows when the groundwater table is not at the surface. For this reason we choose instead to analyze average k values which are obtained through integration of the power function over the minimum and maximum values of depth. Figure 9 presents the average hydraulic conductivity in logarithmic space (Log kave) for models calibrated using the lower 20% of data. The results include kw and hsB models with one, three, and ten hillslopes, and uniform and variable parameters. The kw and hsB models with uniform parameters show similar Log kave values with or without partitioning. When M8 is modeled with more hillslopes with variable parameters, we observe a wider range of hydraulic conductivity values, indicating that the models fit observed streamflows by varying the contributions from different hillslopes. The variation among the kave values is within one degree of magnitude for models with uniform parameters, and most values are between two to three degrees of magnitude for models with variable parameters. Most of these variations are within the range reported in previous studies involving M8 which estimated saturated hydraulic conductivity values between 10 and 300 mm/h at this watershed [*McGlynn*, 2002]. Models with ten hillslopes and variable parameters show the largest range of parameter variation.

[38] When comparing Log kave values between models with uniform parameters but calibrated with varying ranges of data, we observe (as shown in Figure 10) that the values increase as the calibration range becomes larger. Larger kave values help the models to simulate larger storm events. Models with ten hillslope partitions and calibrated with the lower 50% of streamflows show values that are similar to models calibrated with the full range. We have seen this before in Figure 7b when these models showed a R_{eff} value
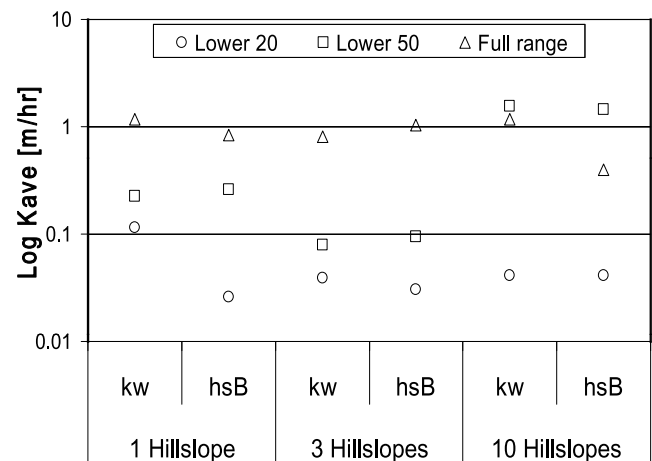
Figure 10. Average hydraulic conductivity (Kave) for kw and hsB models with uniform parameters.

similar to models with variable parameters. This may be an indication that the effective hydraulic conductivity is in fact higher than the values calibrated with models with less partitioning. A further explanation may be that with ten hillslopes partitioning, combined with the larger storms below the 50th percentile, the model have enough flexibility to simulate relatively well over the full range. The parameter range applied during model calibration using a lower percent of streamflows is important because in our experience if the values are very far off from the conceptually realistic [*Sorooshian et al.*, 1983] range a model may perform well at the lower range of data but will do very poorly to simulate the entire hydrograph.

7. Summary and Conclusions

[39] Most studies in the literature related to hillslope storage model applications are based on evaluating model performance on idealized hillslopes and simulated watersheds. Watersheds in the real world, however, often present more complex hillslope and hydrogeologic characteristics making the modeling of these processes a major challenge in hydrological research [*Montanari and Uhlenbrook*, 2004]. One approach to accommodate heterogeneity and varying topographic characteristics that determine hydrological response across a watershed is to partition the watershed into smaller hillslopes. In practical terms the tradeoff between the number of hillslopes, degree of hillslope simplicity (or complexity), number of parameters and respective ranges for calibration, available data, and required computational time continues to be an issue in watershed modeling.

[40] For the present analysis the kinematic wave hillslope storage (kw) and the hillslope storage Boussinesq (hsB) models are applied to the Maimai M8 catchment, a relatively small, homogeneous, steep, well studied watershed in New Zealand. A model framework is developed with M8 partitioned into one, three, and ten hillslopes and the models applied using uniform and variable parameters across the watershed. Our results indicate the following:

[41] 1. When simulating the entire streamflow hydrograph over a limited time period, the five-parameter one hillslope model and the five-parameter three hillslope model with uniform parameters performed as well as *Seibert and McDonnell*'s [2002] 16-parameter three-box model. The 13-parameter three hillslope model with variable parameters performed even better than these models.

[42] 2. In general, the kw and hsB models performed similarly. This result was expected since the kw and hsB models should perform similarly under steep hillslopes such as those found at Maimai, where gravity is a major driver for groundwater flow.

[43] 3. When the watershed is modeled with uniform parameters, increasing the number of hillslopes from 1 to multiple produced model improvements in simulating the entire streamflow hydrograph. However, no significant improvements were observed in terms of simulating the lower quantiles. Also, going from three to ten hillslope partitioning did not lead to different results. This indicates that for this watershed, even though hydrogeologic properties are somewhat homogeneous, it is important to allow for variations in topography across the watershed.

[44] 4. When variable parameters are allowed, the compensating effect of heterogeneous divergent and convergent hillslopes allowed flexibility for all models to perform better. The increase in the number of hillslopes with variable parameters improved model simulations for both the lower 20 and 50% of streamflow. However, variable parameter models showed similar performance as the ten hillslope uniform parameter model when simulating the streamflow hydrograph for the models calibrated using the lower 50% of streamflow.

[45] 5. Model predictions of the 30-day annual minimum flow, Q_{30}, were good for a relatively wet year, while all models overestimated Q_{30} for a dry year, suggesting that it is important that the streamflow range for calibration be similar to the streamflow values being predicted, as the calibration process is often driven by the largest events.

[46] 6. The hydraulic conductivity, k, for the kw and hsB models with uniform parameters is similar for models calibrated over the lower 20% of streamflows, but it increases as the calibration range becomes larger. For the models with variable parameters the range of k values increases with the number of hillslope partitions. This indicates that the models with multiple hillslopes fit streamflows by developing a combination of fast and slow draining hillslopes, which may not represent actual hillslope processes. Soft data such as that employed by *Seibert and McDonnell* [2002] might improve the model ability to describe these hydrologic processes.

[47] The results presented here are somewhat limited, as we applied the kw and hsB models to a relatively small watershed with a short record length. Our next steps are to investigate the hsB and kw models in a much larger and more heterogeneous watershed, with some shallower sloped hillslopes and a longer record length. This will allow us to better understand the tradeoffs between hillslope-based model complexity and performance, and the ability of these models to predict low-streamflow characteristics in larger watersheds.

References

Bergstrom, S. (1995), The HBV model, in *Computer Models of Watershed Hydrology*, edited by V. P. Singh, pp. 443–476, Water Resour. Publ., Highlands Ranch, Colo.

Beven, K. J. (1981), Kinematic subsurface stormflow, *Water Resour. Res.*, 17(5), 1419–1424.

Beven, K. J. (2001), Towards an alternative blueprint for a physically based digitally simulated hydrologic response modelling system, *Hydrol. Process.*, 6, 189–206.

Bogaart, P. W., and P. A. Troch (2004), On the use of soil-landscape evolution modelling in understanding the hillslope hydrological response, in *Hydrology: Science and Practice for the 21st Century*, vol. 1, pp. 251–259, Br. Hydrol. Soc., London.

Boussinesq, J. (1903), Sur le débit, en temps de sécheresse, d'une source alimentée par une nappe d'eaux d'infiltration, *C. R. Hebd. Seances Acad. Sci.*, 136, 1511–1517.

Boussinesq, J. (1904), Recherches théoriques sur l'écoulement des nappes d'eau infiltrées dans le sol et sur le débit des sources, *J. Math. Pures Appl.*, *5*(10), 5–78.

Brutsaert, W. (1994), The unit response of groundwater outflow from a hillslope, *Water Resour. Res.*, *30*(10), 2759–2763, doi:10.1029/94WR01396.

Brutsaert, W., and A. I. El-Kadi (1984), The relative importance of compressibility and partial saturation in unconfined groundwater flow, *Water Resour. Res.*, *20*, 400–408, doi:10.1029/WR020i003p00400.

Brutsaert, W., and J. L. Nieber (1977), Regionalized drought flow hydrographs from a mature glaciated plateau, *Water Resour. Res.*, *13*, 637–643, doi:10.1029/WR013i003p00637.

Burnash, R. J. C. (1995), The NWS river forecast system—Catchment modeling, in *Computer Models of Watershed Hydrology*, edited by V. P. Singh, pp. 311–366, Water Resour. Publ., Highlands Ranch, Colo.

Chapman, T. J. (1995), Comment on "The unit response of groundwater outflow from a hillslope" by Wilfried Brutsaert, *Water Resour. Res.*, *31*(9), 2377–2378, doi:10.1029/95WR01488.

Childs, E. (1971), Drainage of groundwater resting on a sloping bed, *Water Resour. Res.*, *7*, 1256–1263, doi:10.1029/WR007i005p01256.

Clausen, B., and C. P. Pearson (1995), Regional frequency analysis of annual maximum streamflow drought, *J. Hydrol.*, *173*, 111–130, doi:10.1016/0022-1694(95)02713-Y.

Duan, Q. Y., V. K. Gupta, and S. Sorooshian (1993), Shuffled complex evolution approach for effective and efficient global minimization, *J. Optim. Theory Appl.*, *76*(3), 501–521, doi:10.1007/BF00939380.

Eltahir, E. A. B. (1992), Drought frequency analysis of annual rainfall series in central and western Sudan, *Hydrol. Sci. J.*, *37*(3), 185–199.

Fan, Y., and R. L. Bras (1998), Analytical solutions to hillslope subsurface storm flow and saturation overland flow, *Water Resour. Res.*, *34*(4), 921–927, doi:10.1029/97WR03516.

Feldman, A. D. (1995), HEC-1 flood hydrograph package, in *Computer Models of Watershed Hydrology*, edited by V. P. Singh, pp. 119–150, Water Resour. Publ., Highlands Ranch, Colo.

Freer, J., J. McDonnell, K. J. Beven, D. Brammer, D. Burns, R. P. Hooper, and C. Kendal (1997), Topographic controls on subsurface storm flow at the hillslope scale for two hydrologically distinct small catchments, *Hydrol. Processes*, *11*(9), 1347–1352, doi:10.1002/(SICI)1099-1085(199707)11:9<1347::AID-HYP592>3.0.CO;2-R.

Freeze, R. A., and J. A. Cherry (1979), *Groundwater*, Prentice-Hall, Englewood Cliffs, N. J.

Frick, D. M., D. Bode, and J. D. Salas (1990), Effect of drought on urban water supplies, I: Drought analysis, *J. Hydraul. Eng.*, *116*(6), 733–753, doi:10.1061/(ASCE)0733-9429(1990)116:6(733).

Haith, D. A., R. Mandel, and R. S. Wu (1992), *GWLF: Generalized Watershed Loading Functions, version 2.0, user's manual*, Cornell Univ., Ithaca, N. Y.

Hilberts, A. G. J., E. E. Van Loon, P. A. Troch, and C. Paniconi (2004), The hillslope-storage Boussinesq model for non-constant bedrock slope, *J. Hydrol.*, *291*, 160–173, doi:10.1016/j.jhydrol.2003.12.043.

Huyakorn, P. S., and G. F. Pinder (1983), *Computational Methods in Subsurface Flow*, Academic, San Diego, Calif.

Kroll, C. N., J. Luz, B. Allen, and R. M. Vogel (2004), Developing a Watershed Characteristics Database to improve low streamflow prediction, *J. Hydrol. Eng.*, *9*(2), 116–125, doi:10.1061/(ASCE)1084-0699(2004)9:2(116).

Lyon, S. W., and P. A. Troch (2007), Hillslope subsurface flow similarity: Real-world tests of the hillslope Peclet number, *Water Resour. Res.*, *43*, W07450, doi:10.1029/2006WR005323.

McDonald, M. G., and A. W. Harbaugh (1988), *A Modular Three-Dimensional Finite-Difference Ground-Water Flow Model*, *U.S. Geol. Surv. Tech. Water Resour. Invest.*, Book 6, Chap. A1, 586 pp.

McDonnell, J. J. (1990), A rationale for old water discharge through macropores in a steep, humid catchment, *Water Resour. Res.*, *26*(11), 2821–2832.

McGlynn, B. L. (2002), Characterizing hillslope-riparian-stream interactions: A scaling perspective, Maimai, New Zealand, State Univ. of N. Y. Coll. Of Environ. Sci. and For., Syracuse.

McGlynn, B. L., J. J. McDonnell, and D. D. Brammer (2002), A review of the evolving perceptual model of hillslope flowpaths at the Maimai catchments, *N. Z. J. Hydrol.*, *257*, 1–26, doi:10.1016/S0022-1694(01)00559-5.

McGlynn, B. L., J. J. McDonnell, J. Seibert, and C. Kendall (2004), Scale effects on headwater catchment runoff timing, flow sources, and groundwater-streamflow relations, *Water Resour. Res.*, *40*, W07504, doi:10.1029/2003WR002494.

Metcalf and Eddy, Inc. (1991), *Wastewater Engineering—Treatment, Disposal, and Reuse*, 3rd ed., McGraw-Hill, New York.

Montanari, A., and S. Uhlenbrook (2004), Catchment modelling: Towards an improved representation of the hydrological processes in real-world model applications, *J. Hydrol.*, *291*, 159, doi:10.1016/j.jhydrol.2003.12.035.

Mosley, M. (1979), Streamflow generation in a forested watershed, New Zealand, *Water Resour. Res.*, *15*, 795–806, doi:10.1029/WR015i004p00795.

Nash, J. E., and J. V. Sutcliffe (1970), River flow forecasting through conceptual models, part 1—A discussion of principles, *J. Hydrol.*, *10*, 282–290, doi:10.1016/0022-1694(70)90255-6.

Paniconi, C., P. A. Troch, E. E. van Loon, and A. G. J. Hilberts (2003), Hillslope-storage Boussinesq model for subsurface flow and variable source areas along complex hillslopes: 2. Intercomparison with a three-dimensional Richards equation model, *Water Resour. Res.*, *39*(11), 1317, doi:10.1029/2002WR001730.

Pearce, A., M. Stewart, and M. Sklash (1986), Storm runoff generation in humid headwater catchments: 1. Where does the water come from?, *Water Resour. Res.*, *22*, 1263–1272, doi:10.1029/WR022i008p01263.

Polubarinova-Kochina, P. Y. (1962), *Theory of Groundwater Movement*, translated from Russian by DeWiest, R. J. M., 613 pp., Princeton Univ. Press, Princeton, N. J.

Quick, M. C. (1995), The UBC watershed model, in *Computer Models of Watershed Hydrology*, edited by V. P. Singh, pp. 233–280, Water Resour. Publ., Highlands Ranch, Colo.

Rowe, L. K. (1979), Rainfall interception by a beech-podocarp-hardwood forest near Reefton, north Westland, *N. Z. J. Hydrol.*, *18*, 63–72.

Rowe, L. K., A. J. Pierse, and C. L. O'Loughlin (1994), Hydrology and related changes after harvesting native forest catchments and establishing *Pinus radiata* plantations, part 1. Introduction to the study, *Hydrol. Processes*, *8*, 263–279.

Rupp, D. E., and J. S. Selker (2006), On the use of the Boussinesq equation for interpreting recession hydrographs from sloping aquifers, *Water Resour. Res.*, *42*, W12421, doi:10.1029/2006WR005080.

Seibert, J., and J. J. McDonnell (2002), On the dialog between experimentalist and modeler in catchment hydrology: Use of soft data for multi-criteria model calibration, *Water Resour. Res.*, *38*(11), 1241, doi:10.1029/2001WR000978.

Shin, H.-S., and J. D. Salas (2000), Regional drought analysis based on neural networks, *J. Hydrol. Eng.*, *5*(2), 145–155, doi:10.1061/(ASCE)1084-0699(2000)5:2(145).

Snow, D. T. (1969), Anisotropic permeability of fractured media, *Water Resour. Res.*, *5*(6), 1273–1289, doi:10.1029/WR005i006p01273.

Sorooshian, S., V. K. Gupta, and J. L. Fulton (1983), Evaluation of maximum likelihood parameter estimation techniques for conceptual rainfall-runoff models: Influence of calibration data variability and length on model credibility, *Water Resour. Res.*, *19*(1), 251–259, doi:10.1029/WR019i001p00251.

Sorooshian, S., and V. K. Gupta (1995), Model calibration, in *Computer Models of Watershed Hydrology*, edited by V. P. Singh, pp. 23–68, Water Resour. Publ., Highlands Ranch, Colo.

Stedinger, J. R., and W. O. Thomas Jr. (1985), Low-flow frequency estimation using base-flow measurements, *U. S. Geol. Surv. Open File Rep.*, 85–95.

Stefano, C. D., V. Ferro, P. Porto, and G. Tusa (2000), Slope curvature influence on soil erosion and deposition process, *Water Resour. Res.*, *36*(2), 607–617, doi:10.1029/1999WR900157.

Sugawara, M. (1995), Tank model, in *Computer Models of Watershed Hydrology*, edited by V. P. Singh, pp. 165–214, Water Resour. Publ., Highlands Ranch, Colo.

Tallaksen, L. M. (1995), A review of baseflow recession analysis, *J. Hydrol.*, *165*, 349–370, doi:10.1016/0022-1694(94)02540-R.

Troch, P., A. van Loon, and A. Hilbert (2002), Analytical solutions to a hillslope-storage kinematic wave equation for subsurface flow, *Adv. Water Resour.*, *25*(6), 637–649, doi:10.1016/S0309-1708(02)00017-9.

Troch, P., C. Paniconi, and E. E. van Loon (2003), Hillslope-storage Boussinesq model for subsurface flow and variable source areas along complex hillslopes: 1. Formulation and characteristic response, *Water Resour. Res.*, *39*(11), 1316, doi:10.1029/2002WR001728.

Vogel, R. M., and N. M. Fennessey (1995), Flow duration curves II: A review of applications in water resources planning, *Water Resour. Bull.*, *31*(6), 1029–1039.

Vogel, R. M., and C. N. Kroll (1992), Regional geohydrologic-geomorphic relationships for the estimation of low-flow statistics, *Water Resour. Res.*, *28*(9), 2451–2458, doi:10.1029/92WR01007.

Wang, H. F., and M. P. Anderson (1982), *Introduction to Groundwater Modeling: Finite Difference and Finite Element Methods*, Academic, San Diego, Calif.

Weiler, M., B. L. McGlynn, K. J. Beven, and J. J. McDonnell (2003), How does rainfall become runoff? A combined tracer and runoff transfer function approach, *Water Resour. Res.*, *39*(11), 1315, doi:10.1029/2003WR002331.

Wooding, R. A., and T. G. Chapman (1966), Groundwater flow over a sloping impermeable layer: 1. Application of the Dupuit-Forchkeimer assumption, *J. Geophys. Res.*, *71*(12), 2895–2902.

Yeh, G. T. (1987), FEMWATER: A finite element model of water flow through saturated-unsaturated porous media—First revision, Rep. 2943, Environ. Sci. Div., Oak Ridge Natl. Lab., Oak Ridge, Tenn.

Zhang, Z., and C. N. Kroll (2007a), A closer look at baseflow correlation, *J. Hydrol. Eng.*, *12*(2), 190–196, doi:10.1061/(ASCE)1084-0699(2007)12:2(190).

Zhang, Z., and C. N. Kroll (2007b), The baseflow correlation method with multiple gauged sites, *J. Hydrol.*, *347*(3–4), 371–380, doi:10.1016/j.jhydrol.2007.09.025.

C. Kroll and A. H. Matonse, Department of Environmental Resources and Forest Engineering, State University of New York College of Environmental Science and Forestry, Syracuse, NY 13210, USA. (cnkroll@esf.edu)